

Two-photon transport through a waveguide coupling to a whispering gallery resonator containing an atom and photon-blockade effect

T. Shi¹ and Shanhui Fan²

¹*Max-Planck-Institut für Quantenoptik, Hans-Kopfermann-Str. 1, 85748 Garching, Germany*

²*Ginzton Laboratory, Department of Electrical Engineering,
Stanford University, Stanford, California 94305, USA*

(Dated: August 8, 2012)

We investigate the two-photon transport through a waveguide side-coupling to a whispering-gallery-atom system. Using the Lehmann-Symanzik-Zimmermann (LSZ) reduction approach, we present the general formula for the two-photon processes including the two-photon scattering matrices, the wavefunctions and the second order correlation functions of the out-going photons. Based on the exact results of the second order correlation functions, we analyze the quantum statistics behaviors of the out-going photons for two different cases: (a) the ideal case without the inter-modal coupling in the whispering gallery resonator; (b) the case in the presence of the inter-modal coupling which leads to more complex nonlinear behavior. In the ideal case, we show that the system consists of two independent scattering pathways, a free pathway by a cavity mode without atomic excitation, and a "Jaynes-Cummings" pathway described by the Jaynes-Cummings Hamiltonian of a single-mode cavity coupling to an atom. The free pathway does not contribute to correlated two-photon processes. In the presence of intermodal mixing, the system no longer exhibits a free resonant pathway. Instead, both the single-photon and the two-photon transport properties depend on the position of the atom. Thus, in the presence of intermodal mixing one can in fact tune the photon correlation properties by changing the position of the atom. Our formalism can be used to treat resonator and cavity dissipation as well.

PACS numbers: 42.50.-p, 42.79.Gn, 11.55.Ds

I. INTRODUCTION

Recently, the whispering-gallery-atom system inspires a lot of interest [1–11], owing to its broad applications in the studies of quantum optics. A schematic of such a system are shown in Fig. 1, where a waveguide is side-coupled to a whispering-gallery resonator, which then couples to a two-level system. In the experimental study of this system [2–4], the two-level system can be either a quantum dot [2], or an actual atom [3]. Here, we will refer such a two-level system as an "atom". These experiments have measured the transmission properties of such a waveguide-resonator-atom system under weak light excitation, and have demonstrated quantum effects including anti-bunching and photon blockade effects.

The experimental progress on this system, in turn, motivated several recent theoretical studies. Srinivasan and Painter analyzed this system under the excitation of a weak coherent state input [12], and obtained transmission properties and coherence properties of the transmission through a numerical procedure with a truncated number-state basis for the photons in the resonator [5]. Shen and Fan calculated analytically the transmission properties of such a resonator system with an input of a single-photon Fock state [6, 7]. Subsequently, the single-photon transports in the whispering-gallery system have been extensively studied [8–11].

In this paper, we study the two-photon transport property of this system shown in Fig. 1. While the response of the system under weak coherent-state input yields much

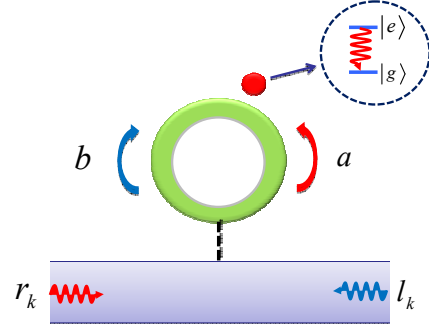


FIG. 1: (Color online) The schematics for the system: The blue and red arrows denote the two whispering-gallery modes, which interact with the atom and the waveguide.

information about its non-classical properties, we note that one important goal of integrated quantum optics is to process quantum states. Therefore, it is important to study such a system with the input of non-classical states such as Fock state as well. In addition, in contrast to the study of the transport properties of a single photon [13–18], the studies of two-photon transports provide important information [19–26] about atom-induced photon-photon interaction that is absent in the single-photon Hilbert space. Of particular interest is the anti-bunching behavior of the two outgoing photons, which indicate the photon blockade effects [24], as has been observed in a variety of systems [27–40].

The paper is organized as follows. In Sec. II we review the model Hamiltonian and our theoretical approach based on the Lehmann-Symanzik-Zimmermann (LSZ) reduction formula in quantum field theory [41]. This approach results in an exact formula for the scattering matrix of the system in multi-photon sub-space. In Sec. III, we present the exact analytical results, including the single-photon transmissions and the wavefunctions for the two out-going photons. Based on the general analytical results, we analyze the very distinct quantum statistics behaviors of the out-going photons for two different cases in Sec. IV and Sec. V. Section IV considers the ideal case in the absence of inter-modal coupling in the whispering gallery resonator. Section V analyzes the effect of inter-modal coupling which leads to more complex nonlinear behavior. In Sec. VI, the results are summarized with some remarks and outlooks.

II. MODEL SETUP

The system in Fig. 1 is described by the Hamiltonian [6, 7]

$$H = H_W + H_{wg} + H_{hyb}. \quad (1)$$

Here,

$$H_W = \sum_{k>0} k r_k^\dagger r_k - \sum_{k<0} k l_k^\dagger l_k \quad (2)$$

describes photons propagating in the waveguide. r_k (r_k^\dagger) and l_k (l_k^\dagger) are the annihilation (creation) operators of right-moving and left-moving photons, respectively. The right-moving photons have momentum $k > 0$, and the left-moving photons have momentum $k < 0$.

In Eq. (1)

$$H_{wg} = \Omega |e\rangle \langle e| + \omega_c (a^\dagger a + b^\dagger b) + h b^\dagger a + h^* a^\dagger b + \sigma^+ (g_a a + g_b b) + \text{H.c.} \quad (3)$$

describes the two-level system, the resonator, and the interaction between them under the rotating-wave approximation. In Eq. (3), a and b are the annihilation operators for the two counter rotating modes in the resonator. h is the strength of intermodal-coupling between these two modes and is typically induced by surface roughness on the resonator. The atom supports a ground state $|g\rangle$ and an excited state $|e\rangle$ with a transition frequency Ω . g_a (g_b) is the coupling constant between mode a (b) and the atom, and $\sigma^+ = |e\rangle \langle g|$.

In Eq. (1),

$$H_{hyb} = \frac{1}{\sqrt{L}} \sum_k (V_R r_k^\dagger a + V_L l_k^\dagger b + \text{H.c.}) \quad (4)$$

describes the coupling between the waveguide and the resonator. Here, we adopt a box-normalization scheme with L being the length of the waveguide, and V_R (V_L)

is the coupling strength between the right-moving (left-moving) photon in the waveguide and the mode a (b) in the whispering-gallery system.

We end this section by briefly commenting on various experimental aspects that are related to the Hamiltonian of Eq. (1). As a representative example, the experiment in Refs. [2–4] has $\omega_c \sim \Omega \sim 10^6 \text{GHz}$. The resonator linewidth $\Gamma/2\pi = 0.1 \sim 10 \text{MHz}$. The atom-resonator coupling constant $|g_i|/2\pi$ ($i = a, b$) can reach $10 \text{MHz} \sim 10 \text{GHz}$. While our theory does not depend on such a detailed choice of parameters, in the numerical examples below we will be focusing on a similar strong-coupling regime where $|g_i| \gg \Gamma$.

In the experiment in Refs. [3] the intermodal mixing has a strength of $|h|/2\pi = 1 \sim 100 \text{MHz}$. The phase of the h depends on the detail of the surface roughness and typically cannot be controlled in an experiment. On the other hand, the relative phase of g_a and g_b depends on the position of the atom, which can be controlled experimentally [6, 7]. Since the size of the whispering gallery mode is at least a few wavelength, the relative phase of g_a and g_b can vary anywhere between 0 and 2π .

III. OVERVIEW OF THE THEORETICAL APPROACH

We solve the single- and two-photon scattering matrix (S -matrix) for the Hamiltonian in Eq. (1) using the LSZ approach. This approach has been discussed in details in Ref. [23, 24]. Here we only provide a brief summary of those aspects that are relevant for subsequent discussions.

The single-photon and two-photon S -matrices read

$$S_{p;k} = \delta_{kp} + iT_{p;k}, \quad (5)$$

and

$$S_{p_1 p_2; k_1 k_2} = S_{p_1 k_1} S_{p_2 k_2} + S_{p_2 k_1} S_{p_1 k_2} + iT_{p_1 p_2; k_1 k_2}, \quad (6)$$

respectively, where k (p) is the momentum of the incident (out-going) single-photon, and k_1, k_2 (p_1, p_2) are the momenta of two incident (out-going) photons. The right and left moving photons have the positive and negative momenta, respectively. Here, the T -matrix element $T_{p_1, \dots, p_n; k_1, \dots, k_n} \equiv T_{[\mathbf{p}; \mathbf{k}]}$ has the form

$$iT_{[\mathbf{p}; \mathbf{k}]} = \lim_{\substack{\omega_{k_j} \rightarrow k_j, \\ \omega_{p_j} \rightarrow p_j}} \frac{(2\pi)^n G_{[\mathbf{p}; \mathbf{k}]}(\omega_{\mathbf{p}}, \omega_{\mathbf{k}})}{\prod_{j=1}^n [G_0(\omega_{k_j}, k_j) G_0(\omega_{p_j}, p_j)]}. \quad (7)$$

In Eq. (7), $G_0(\omega, k) = i/(\omega - \varepsilon_k + i0^+)$ is the free propagator of a single photon with $\varepsilon_k = |k|$ being the dispersion relation of the waveguide.

$$G_{[\mathbf{p}; \mathbf{k}]}(\omega_{\mathbf{p}}, \omega_{\mathbf{k}}) = \int \prod_{j=1}^n \left[\frac{dt_j dt'_j}{2\pi} \right] G_{[\mathbf{p}; \mathbf{k}]}(\mathbf{t}', \mathbf{t}) \times \prod_{j=1}^n [\exp(i\omega_{p_j} t'_j - i\omega_{k_j} t_j)] \quad (8)$$

is the Fourier transform of the exact Green function $G_{[\mathbf{p};\mathbf{k}]}(\mathbf{t}', \mathbf{t})$. Such a Green function can be determined as:

$$G_{[\mathbf{p};\mathbf{k}]}(\mathbf{t}', \mathbf{t}) = \frac{(-)^n \delta^{2n} \ln Z[\eta_k, \eta_k^*]}{\delta \eta_{f,p_1}^*(t'_1) \dots \delta \eta_{f,p_n}^*(t'_n) \delta \eta_{f,k_1}(t_1) \dots \delta \eta_{f,k_n}(t_n)} \Bigg|_{\substack{\eta_{f,k}=0 \\ \eta_{f,k}^*=0}}, \quad (9)$$

where

$$Z[\eta_k, \eta_k^*] = \int D[\text{field}] \exp(iS_c + iS_{\text{ex}}) \quad (10)$$

is the generating functional in the path integral formalism. Here, $\int D[\text{field}]$ denotes the path integral over the all fields in the system, S_c is the action of the system, and

$$S_{\text{ex}} = \sum_{f=r,l} \int dt \sum_k [\eta_{f,k}^*(t) f_k(t) + \text{H.c.}] \quad (11)$$

describes the external sources $\eta_{f,k}(t)$ that injects photons into the waveguide.

Based on the formalism as outlined above, in the next section we show the exact analytical results for the single-photon and two-photon scattering processes.

IV. ANALYTIC RESULTS FOR ONE AND TWO PHOTON S -MATRICES

In this section, the S -matrices are obtained by LSZ reduction, which leads to the exact results of the single-photon transmission and the second order correlation functions of the two out-going photons.

A. Single-photon transport

For the single-photon case, using the T -matrix element (7), the Green function (9), and the generating functional (10), we obtain

$$S_{p;k} = T_k \delta_{p,k} + R_k \delta_{p,-k}, \quad (12)$$

where

$$T_k = 1 - i |V_R|^2 \langle 0 | a \frac{1}{k - H_{\text{eff}}} a^\dagger | 0 \rangle \quad (13)$$

and

$$R_k = -i V_L V_R^* \langle 0 | b \frac{1}{k - H_{\text{eff}}} a^\dagger | 0 \rangle \quad (14)$$

are the transmission and reflection coefficients, respectively. Here,

$$H_{\text{eff}} = \Omega |e\rangle \langle e| + (\omega_c - i \frac{\Gamma_R}{2}) a^\dagger a + (\omega_c - i \frac{\Gamma_L}{2}) b^\dagger b + [hb^\dagger a + \sigma^+(g_a a + g_b b) + \text{H.c.}], \quad (15)$$

is the effective Hamiltonian with $\Gamma_R = |V_R|^2$ and $\Gamma_L = |V_L|^2$ being the decay rates of the two whispering-gallery modes to the waveguide, respectively. Without loss of generality, we consider $\Gamma_R = \Gamma_L \equiv \Gamma$. We notice that the excitation number $N = |e\rangle \langle e| + a^\dagger a + b^\dagger b$ commutes with H_{eff} . Thus, for the single-photon scattering, in the single-excitation subspace as spanned by the basis $\{|e\rangle |0\rangle_a |0\rangle_b, |g\rangle |1\rangle_a |0\rangle_b, |g\rangle |0\rangle_a |1\rangle_b\}$, we represent the effective Hamiltonian as

$$H_{\text{eff}}^{(1)} = \begin{pmatrix} \Omega & g_a & g_b \\ g_a^* & \omega_c - i \frac{\Gamma}{2} & h^* \\ g_b^* & h & \omega_c - i \frac{\Gamma}{2} \end{pmatrix}. \quad (16)$$

Using the form of $H_{\text{eff}}^{(1)}$ in Eq. (16), the single-photon reflection and transmission coefficients can be determined as

$$R_k = \frac{-i V_L V_R^*}{D(k)} [g_a g_b^* + h(k - \Omega)], \quad (17)$$

and

$$T_k = 1 - \frac{i\Gamma}{D(k)} [(k - \Omega)(k - \omega_c + i \frac{\Gamma}{2}) - |g_b|^2], \quad (18)$$

respectively. Here, we define

$$D(k) = (k - \omega_c + i \frac{\Gamma}{2}) [(k - \Omega)(k - \omega_c + i \frac{\Gamma}{2}) - G_+^2] - g_a^* g_b h - g_b^* g_a h^* - |h|^2 (k - \Omega), \quad (19)$$

and

$$G_+ = \sqrt{|g_a|^2 + |g_b|^2}. \quad (20)$$

The results (17) and (18) accord with that obtained in Ref. [6, 7].

Equations (17) and (18) are applicable in the absence of intrinsic atomic or cavity dissipation. In the presence of intrinsic dissipations, the reflection and transmission probabilities $|R_k|^2$ and $|T_k|^2$ are obtained by substitution $\Omega - i\gamma_a$ and $\omega_c - i\gamma_c$ for Ω and ω_c in Eqs. (17) and (18), where γ_a and γ_c are the intrinsic decay rates of the cavity and the atom.

B. Two-photon transport

In the subsection, we derive the exact formula for the scattering wavefunctions and the second order correlation functions of two out-going photons by LSZ reduction approach. By evaluating Eqs. (7), (9) and (10), we obtain the S -matrix elements in the two-photon Hilbert space:

$$S_{p_1 p_2; k_1 k_2}^{(R)} = R_{k_1} R_{k_2} (\delta_{p_1, -k_1} \delta_{p_2, -k_2} + \delta_{p_1, -k_2} \delta_{p_2, -k_1}) - i \frac{V_L^2 V_R^{*2}}{2\pi} \delta_{p_1 + p_2, -k_1 - k_2} U_{p_1 p_2; k_1 k_2}, \quad (21)$$

and

$$S_{p_1 p_2; k_1 k_2}^{(T)} = T_{k_1} T_{k_2} (\delta_{p_1, k_1} \delta_{p_2, k_2} + \delta_{p_1, k_2} \delta_{p_2, k_1}) - i \frac{|V_R|^4}{2\pi} \delta_{p_1 + p_2, k_1 + k_2} W_{p_1 p_2; k_1 k_2}, \quad (22)$$

for two reflected photons and transmitted photons, where R and T refers to transmission and reflection, respectively. In Eqs. (21) and (22),

$$U_{p_1 p_2; k_1 k_2} = F_1(p_1, p_2; k_1, k_2) + F_1(p_1, p_2; k_2, k_1) + F_1(p_2, p_1; k_1, k_2) + F_1(p_2, p_1; k_2, k_1), \quad (23)$$

and

$$W_{p_1 p_2; k_1 k_2} = F_2(p_1, p_2; k_1, k_2) + F_2(p_1, p_2; k_2, k_1) + F_2(p_2, p_1; k_1, k_2) + F_2(p_2, p_1; k_2, k_1). \quad (24)$$

Here, we define

$$F_1(p_1, p_2; k_1, k_2) = \langle 0 | b \frac{1}{-p_1 - H_{\text{eff}}^{(1)}} b \frac{1}{k_1 + k_2 - H_{\text{eff}}^{(2)}} a^\dagger \frac{1}{k_2 - H_{\text{eff}}^{(1)}} a^\dagger | 0 \rangle + \frac{1}{-p_1 - k_1} \langle 0 | b \frac{1}{-p_1 - H_{\text{eff}}^{(1)}} a^\dagger b \frac{1}{k_2 - H_{\text{eff}}^{(1)}} a^\dagger | 0 \rangle, \quad (25)$$

and

$$F_2(p_1, p_2; k_1, k_2) = \langle 0 | a \frac{1}{p_1 - H_{\text{eff}}^{(1)}} a \frac{1}{k_1 + k_2 - H_{\text{eff}}^{(2)}} a^\dagger \frac{1}{k_2 - H_{\text{eff}}^{(1)}} a^\dagger | 0 \rangle + \frac{1}{p_1 - k_1} \langle 0 | a \frac{1}{p_1 - H_{\text{eff}}^{(1)}} a^\dagger a \frac{1}{k_2 - H_{\text{eff}}^{(1)}} a^\dagger | 0 \rangle, \quad (26)$$

where $H_{\text{eff}}^{(1)}$ is defined in Eq. (16). In the two-excitation subspace as spanned by the basis $\{|g\rangle|2\rangle_a|0\rangle_b, |e\rangle|1\rangle_a|0\rangle_b, |g\rangle|1\rangle_a|1\rangle_b, |e\rangle|0\rangle_a|1\rangle_b, |g\rangle|0\rangle_a|2\rangle_b\}$, we represent the effective Hamiltonian

$$H_{\text{eff}}^{(2)} = \begin{pmatrix} 2\alpha & \sqrt{2}g_a^* & \sqrt{2}h^* & 0 & 0 \\ \sqrt{2}g_a & \alpha + \Omega & g_b & h^* & 0 \\ \sqrt{2}h & g_b^* & 2\alpha & g_a^* & \sqrt{2}h^* \\ 0 & h & g_a & \alpha + \Omega & \sqrt{2}g_b \\ 0 & 0 & \sqrt{2}h & \sqrt{2}g_b^* & 2\alpha \end{pmatrix}, \quad (27)$$

where $\alpha = \omega_c - i\Gamma/2$. In general, direct evaluation of $U_{p_1 p_2; k_1 k_2}$ and $W_{p_1 p_2; k_1 k_2}$ can be rather complicated. However, there are cases where $U_{p_1 p_2; k_1 k_2}$ and $W_{p_1 p_2; k_1 k_2}$ can be obtained exactly in a compact form. We will discuss such examples in the next section.

The Fourier transformations of matrix elements (21) and (22) result in wavefunctions of the two reflected or transmitted photons:

$$\begin{aligned} \psi_R(x_1, x_2) &= \frac{1}{4\pi} \int dp_1 dp_2 R_{p_1 p_2; k_1 k_2} e^{ip_1 x_1 + ip_2 x_2} \\ &= \frac{1}{2\pi} e^{-iEx_c} [R_{k_1} R_{k_2} \cos(\Delta_k x) \\ &\quad + \frac{1}{2} V_L^2 V_R^{*2} \int \frac{d\Delta_p}{2\pi i} e^{i\Delta_p x} U_{p_1 p_2; k_1 k_2}], \end{aligned} \quad (28)$$

and

$$\begin{aligned} \psi_T(x_1, x_2) &= \frac{1}{4\pi} \int dp_1 dp_2 T_{p_1 p_2; k_1 k_2} e^{ip_1 x_1 + ip_2 x_2} \\ &= \frac{1}{2\pi} e^{iEx_c} [T_{k_1} T_{k_2} \cos(\Delta_k x) \\ &\quad + \frac{1}{2} |V_R|^4 \int \frac{d\Delta_p}{2\pi i} e^{i\Delta_p x} W_{p_1 p_2; k_1 k_2}], \end{aligned} \quad (29)$$

respectively. Here, we define the total momentum $E = k_1 + k_2 = p_1 + p_2$, the relative momenta $\Delta_k = (k_1 - k_2)/2$ and $\Delta_p = (p_1 - p_2)/2$, as well as the center of mass coordinate $x_c = (x_1 + x_2)/2$ and the relative coordinate $x = x_1 - x_2$. Because $U_{p_1 p_2; k_1 k_2}$ and $W_{p_1 p_2; k_1 k_2}$ are both even functions of Δ_p , $\psi_R(x_1, x_2)$ and $\psi_T(x_1, x_2)$ are invariant under the permutation $x_1 \longleftrightarrow x_2$, as required since photons are bosons. From now on, we only focus on the wavefunctions for $x > 0$.

The integral in Eqs. (28) and (29) can be evaluated by analyzing the analytic properties of the matrix elements $U_{p_1 p_2; k_1 k_2}$ and $W_{p_1 p_2; k_1 k_2}$. These matrix elements exhibit three poles $p_l = E/2 - \alpha_l$ on the upper half plane, where α_l is the eigenvalue of $H_{\text{eff}}^{(1)}$ with $l = 1, 2, 3$. Here, notice that the eigenvalues of $H_{\text{eff}}^{(2)}$ do not contribute to the poles in $U_{p_1 p_2; k_1 k_2}$ and $W_{p_1 p_2; k_1 k_2}$, because they only associate with the total energy E , as shown in Eqs. (25) and (26), and we consider here an incident two-photon state with a fixed total energy. The residue theorem then leads to the wavefunctions

$$\begin{aligned} \psi_R(x_1, x_2) &= \frac{1}{2\pi} e^{-iEx_c} [R_{k_1} R_{k_2} \cos(\Delta_k x) \\ &\quad + \frac{1}{2} V_L^2 V_R^{*2} \sum_l \text{Res}_{p_l} U_{p_1 p_2; k_1 k_2} e^{ip_l x}], \end{aligned} \quad (30)$$

and

$$\begin{aligned} \psi_T(x_1, x_2) &= \frac{1}{2\pi} e^{iEx_c} [T_{k_1} T_{k_2} \cos(\Delta_k x) \\ &\quad + \frac{1}{2} |V_R|^4 \sum_l \text{Res}_{p_l} W_{p_1 p_2; k_1 k_2} e^{ip_l x}], \end{aligned} \quad (31)$$

where $\text{Res}_{p_l} \Phi(\Delta_p)$ denotes the residue of the function $\Phi(\Delta_p)$ at p_l .

From the two-photon wavefunctions, the second-order correlations functions for the reflected and transmitted photons can be obtained as:

$$\begin{aligned} g_R^{(2)}(\tau) &= \frac{\langle \psi_R | l^\dagger(x) l^\dagger(x+\tau) l(x+\tau) l(x) | \psi_R \rangle}{|\langle \psi_R | l^\dagger(x) l(x) | \psi_R \rangle|^2}, \\ g_T^{(2)}(\tau) &= \frac{\langle \psi_T | r^\dagger(x) r^\dagger(x+\tau) r(x+\tau) r(x) | \psi_T \rangle}{|\langle \psi_T | r^\dagger(x) r(x) | \psi_T \rangle|^2}, \end{aligned} \quad (32)$$

where $r(x)$ ($l(x)$) is the Fourier transformation of r_k (l_k). Equation (32) can be simplified to yield $g_s^{(2)}(\tau) = |\psi_s(x+\tau, x)|^2 / \int dy |\psi_s(x, y)|^2$, where s denote ‘‘R’’ and ‘‘T’’. Therefore, our theoretical results on the two-photon

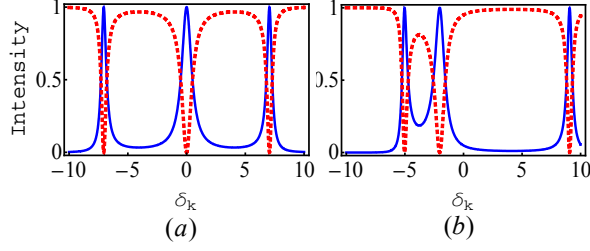


FIG. 3: (Color online) Single photon transmission (Red dashed curve) and reflection (Blue solid curve) spectra for the effective single-mode case. All quantities with energy dimensions are normalized to Γ , δ_k is the detuning between the incident photon and ω_c : (a) $h = 0$, $|g_a| = |g_b| = 5$, and $\Omega = \omega_c$; (b) $|h| = 2$, $|g_a| = |g_b| = 5$, $g_b/g_a = e^{-i\theta_h}$, and the detuning $\Omega - \omega_c = 2$ between atom and the cavity.

A. Single-photon transport

For this effective single-mode case, the single-photon reflection coefficient (14) can be rewritten as

$$R_k = -i \frac{\Gamma g_a g_b^*}{G_+^2} \left[\frac{k - \Omega}{(k - \Omega)(k - \omega_A) - G_+^2} - \frac{1}{k - \omega_B} \right], \quad (37)$$

in which the first and second terms describe the contributions from the JC mode and the free mode, respectively. We show the single-photon reflection and transmission probabilities $|R_k|^2$ and $|T_k|^2$ in Fig. 3. In Fig. 3a, we choose $h = 0$, $\Omega = \omega_c$, and $|g_a| = |g_b|$. We find that in the strong coupling limit $\Gamma \ll G_+$ there are three peaks in the reflection spectrum. The peak in the center of the spectrum corresponds to the free mode B . Two other peaks corresponds to the JC modes in the single-excitation subspace.

In Fig. 3b, we choose $\Omega = \omega_c + |h|$ and $g_b/g_a = e^{-i\theta_h}$. In the strong coupling limit $\Gamma \ll G_+$, the reflection spectrum again exhibits three peaks. The central peak again corresponds to the free mode. Compared to the free mode in Fig. 3a at the frequency ω_c , here the frequency of the free mode is shifted to $\omega_c - |h|$ due to the intermodal coupling. Other two peaks corresponds to the two JC modes.

Based on these results, we conclude that the single-photon transport consists of two independent scattering processes, i.e., the scattering by the JC modes, which have atomic excitation, and by the free mode that is decoupled from the atom.

B. Two-photon transport and photon blockade

For this effective single-mode case, straightforward calculations of Eqs. (25) and (26) lead to the analytic results

$$U_{p_1 p_2; k_1 k_2} = - \frac{2g_b^{*2} g_a^2 (E - \omega_A - \Omega)}{\prod_{s=\pm} (E - \lambda_{2s})} \frac{(E - 2\Omega)(E - 2\omega_A) - 4G_+^2}{\prod_{s=\pm} \prod_{i=1,2} (k_i - \lambda_{1s})(p_i + \lambda_{1s})}, \quad (38)$$

and

$$W_{p_1 p_2; k_1 k_2} = - \frac{2|g_a|^4 (E - \omega_A - \Omega)}{\prod_{s=\pm} (E - \lambda_{2s})} \frac{(E - 2\Omega)(E - 2\omega_A) - 4G_+^2}{\prod_{s=\pm} \prod_{i=1,2} (k_i - \lambda_{1s})(p_i - \lambda_{1s})}. \quad (39)$$

Here, $\lambda_{1\pm}$ and $\lambda_{2\pm}$ are the eigenvalues of H_{JC} in the single- and two-excitation subspaces [24]. We note that $U_{p_1 p_2; k_1 k_2}$ and $W_{p_1 p_2; k_1 k_2}$, i.e., the two-photon correlated scattering, have contributions only from the JC modes. The free mode does not contribute to the correlated scattering since it does not have any atomic excitation.

In Fig. 4, the two-photon background fluorescence $B_R = |V_R|^4 |V_L|^4 |U_{p_1 p_2; k_1 k_2}|^2 / 4\pi^2$ of the reflected photons are shown for the strong coupling limit $G_+ \gg \Gamma$. The two-photon background fluorescence displays a single peak at $\Delta_k = \Delta_p = 0$ when the total energy of the incident photons approaches $2\text{Re}\lambda_{1\pm}$ (Fig. 4a and b), while the two-photon background fluorescence splits into four peaks when the total energy of the incident photons deviates from $2\text{Re}\lambda_{1\pm}$ (Fig. 4c and d).

In general, the background fluorescence peaks when one of the incident or outgoing photons has energy that coincides with a single-excitation eigenstate [24]. Examining Eqs. (38) and (39), we see that the poles occur at $\Delta_k = \pm(E/2 - \text{Re}\lambda_{1s})$ and $\Delta_p = \pm(E/2 - \text{Re}\lambda_{1s})$. Thus, one might expect eight peaks in the background fluorescence spectra in the general case. However, four of these poles turn out to have very small residues, resulting in the presence of only four peaks in Figs. 4c and d.

Together with Eqs. (38) and (39), it follows from Eqs. (30) and (31) that the outgoing two-photon wavefunctions are

$$\psi_R(x_1, x_2) = \frac{e^{-iEx_c}}{2\pi} [R_{k_1} R_{k_2} \cos(\Delta_k x) - V_L^2 V_R^{*2} g_b^{*2} g_a^2 F(x)], \quad (40)$$

and

$$\psi_T(x_1, x_2) = \frac{e^{iEx_c}}{2\pi} [T_{k_1} T_{k_2} \cos(\Delta_k x) - |V_R|^4 |g_a|^4 F(x)], \quad (41)$$

of the reflected and transmitted photons, respectively, where we define

$$F(x) = \frac{\sum_s s(E - 2\lambda_{1s}) e^{i(\frac{E}{2} - \lambda_{1-s})|x|}}{\prod_{s=\pm} [(E - \lambda_{2s}) \prod_{i=1,2} (k_i - \lambda_{1s})] (\lambda_{1+} - \lambda_{1-})}. \quad (42)$$

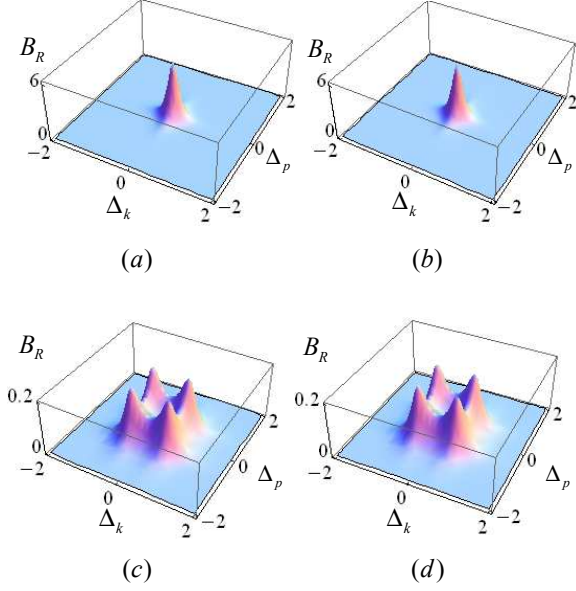


FIG. 4: (Color online) The two-photon background fluorescence for the effective single-mode case. All quantities with dimension of energy are normalized with respect to Γ : (a) The system parameters are the same as those in Fig. 3(a), and the detuning $E - 2\omega_c = -14$; (b) The system parameters are the same as those in Fig. 3(b), and the detuning $E - 2\omega_c = -10$; (c) The system parameters are the same as those in Fig. 3(a), and the detuning $E - 2\omega_c = 13$; (d) The system parameters are the same as those in Fig. 3(b), and the detuning $E - 2\omega_c = 17$.

In Fig. 5, we plot the second-order correlation for the two reflected photons, as obtained by applying Eq. (32) to the wavefunctions determined from Eqs. (40) and (41). Here, we consider the same two systems in Fig. 3, and assume that the two incident photons have the same single-photon energy of $E/2$. In Fig. 3, we saw that the systems exhibit strong resonant reflection for single photon, when the single-photon energy is resonant with either the JC modes or the free modes. However, in the presence of two incident photons, the statistics of the outgoing photons at these resonances are very different. As we see in Fig. 5, when the single-photon energy coincides with the energy of one of JC modes, e.g., $E/2 - \omega_c \sim -7$ in Fig. 5c and $E/2 - \omega_c \sim -5$ in Fig. 5d, we observe pronounced anti-bunching behavior with $g_R^{(2)}(0) < g_R^{(2)}(\tau) \leq 1$, and therefore a strong photon-blockade effect. On the other hand, no anti-bunching behavior or photon blockade effect is observed when the single-photon energy coincides with that of the free mode, e.g., $E/2 - \omega_c \sim 0$ in Fig. 5c and $E/2 - \omega_c \sim -2$ in Fig. 5d.

The presence or absence of photon blockade effect at the different resonances is closely related to energy spectrum as we analyzed in Figs. 2a and b. Since the free mode B is decoupled from the atom, its energy spectrum $E = n(\omega_c \mp |h|)$ is linear. Thus, there is no photon blockade effect when the incident photon is resonant with the

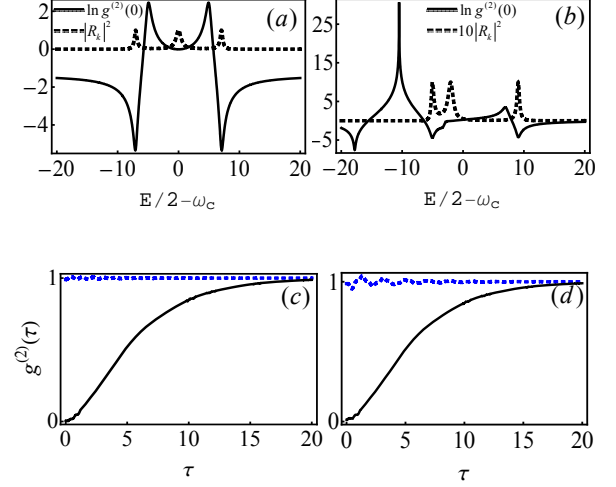


FIG. 5: (Color online) The second order correlation functions of two reflected photons for the effective single-mode case. The two incident photons have the same energy $E/2$. All quantities with dimension of energy are normalized with respect to Γ , and the system parameters for the left and the right panels are the same as those in Fig. 3(a) and (b), respectively. In (a) and (b), the second order correlation function and the reflection coefficient are depicted by the solid and dashed curves, respectively. (c) The solid (black) and dashed (blue) curves denote $g_R^{(2)}(\tau)$ for $E/2 - \omega_c = \pm 7$ (single photon being resonant with the JC mode) and $E/2 - \omega_c = 0$ (single photon being resonant with the JC mode), respectively. (d) The solid (black) and blue (dashed) curves denote $g_R^{(2)}(\tau)$ for $E/2 - \omega_c = -5, 9$ (single photon being resonant with the JC mode) and $E/2 - \omega_c = -2$ (single photon being resonant with the JC mode), respectively.

free mode. On the other hand, the spectrum of the JC mode is highly non-linear. Thus, while a single-photon on resonance with one of the JC modes is reflected, two such photons can not be simultaneously reflected since the total energy is off resonance in the two-excitation subspace.

VI. RESULTS FOR THE TWO-MODE CASE

In this section, we use the general formula derived in Sec. III to study the single- and two-photon transports for the two-mode case. In the presence of the intermodal coupling, i.e., $h \neq 0$, we see in Eq. (34) that except for a very special choice of the relative phase of g_a and g_b , corresponding to one special choice of atom position, in general one can not form a photon mode that decouples from the atom. We define $\theta_0 = \arg(g_b/g_a)$. The analytic results for the single-photon intensity response function, and the two-photon correlation function, depends only on $\theta_0 + \theta_h$. Thus, in the numerical results, without loss of generality we fix $\theta_h = \pi/2$, and vary θ_0 from 0 to 2π .

In the two-mode case, where atom couples to two pho-

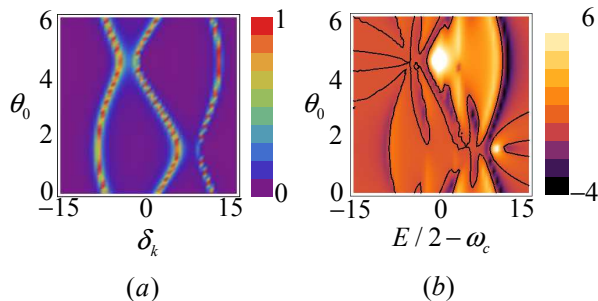


FIG. 6: (Color online) The single photon reflection and the second order correlation functions, where Γ is taken as units, $|h| = 5$, $\theta_h = \pi/2$, and other parameters are the same as those in Fig. 3(b): (a) The single photon reflection; (b) The second order correlation functions $\ln g_R^{(2)}(0)$. Here, the black curves denote $g_R^{(2)}(0) = 1.0$.

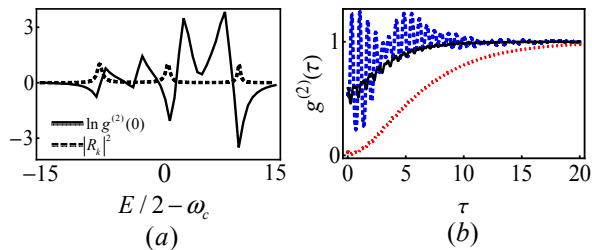


FIG. 7: (Color online) The second order correlation functions of two reflective photons, where $|h| = 5$, $\theta_h = \pi/2$, $\theta_0 = 0$, and Γ is taken as units: (a) The solid and dashed curves denote $\ln g_R^{(2)}(0)$ and the single photon reflection; (b) The solid (black), dashed (blue) and dotted (red) curves denote the $g_R^{(2)}(\tau)$ for the incident resonant energies $E/2 - \omega_c = -7.39, 1$ and 10.84 , respectively. Other parameters are the same as those in Fig. 3(b).

ton modes, both the single photon reflection (Fig. 6a), and in the two-photon case the statistics of the outgoing photon (Fig. 6b), becomes dependent upon θ_0 , and hence the position of the atom. Therefore, by controlling the position of the atom, one can tune both the single-photon

transport and two-photon correlation properties.

Similar to the effective one-mode case, here with the choice of parameters that place the system in the strong-coupling regime, the single-photon reflection also exhibits three peaks (Fig. 7a, dashed line). Unlike the effective one-mode case, however, here all three peaks exhibit photon blockade effect. In Fig. 7b, we plot $g^{(2)}(0)$ for the two reflected photons, when two photons having the same energy $E/2$ are incident upon the system. We see strong resonant behavior of $g^{(2)}(0)$ at the energy corresponding to the three single-photon eigenmodes. The $g^{(2)}(\tau)$ at these three energies are plotted in Fig. 7c, where we see strong photon blockade effect with $g^{(2)}(0) \ll 1$. In the two-mode case, all eigenmodes have atom excitation, and hence contributes to correlated transport.

VII. FINAL REMARK AND CONCLUSION

As a final remark, in the numerical examples we have focused on the case where there is no intrinsic dissipation of either the atom or the cavity. In general, the dissipations suppress the single-photon reflection and the photon blockade effect. We expect that due to the small decay rates of the whispering-gallery system to the environment, the photon blockade effect is well-protected.

In summary, in this paper we study the two-photon transport of the whispering-gallery-atom system by LSZ reduction approach. We consider the cases of systems with or without intermodal mixing, and present exact results on the second-order correlation functions of the two reflected photons, which exhibit photon-blockade effect. We expect the LSZ formalism may be developed to treat photon-blockade effect in other systems as well, including the opto-mechanical system that was considered in [42–45].

Acknowledgments

Tao Shi was supported by the EU project AQUITE. Shanhui Fan acknowledges the support of an AFOSR-MURI program on quantum metamaterial.

-
- [1] M. Rosenblit, P. Horak, S. Helsenby, and R. Folman, Phys. Rev. A **70**, 053808 (2004).
 - [2] K. Srinivasan and O. Painter, Nature (London) **450**, 862 (2007).
 - [3] B. Dayan, A. S. Parkins, T. Aoki, E. P. Ostby, K. J. Vahala, and H. J. Kimble, Science **319**, 1062 (2008).
 - [4] T. J. Kippenberg, S. M. Spillane, and K. J. Vahala, Appl. Phys. Lett. **85**, 6113 (2004).
 - [5] K. Srinivasan and O. Painter, Phys. Rev. A **75**, 023814 (2007).
 - [6] J. T. Shen and S. Fan, Phys. Rev. A **79**, 023838 (2009).
 - [7] J. T. Shen and S. Fan, Phys. Rev. A **82**, 021802(R) (2010).
 - [8] E. E. Hach, III, A. W. Elshaari, and S. F. Preble, Phys. Rev. A **82**, 063839 (2010).
 - [9] X. Zang and C. Jiang, J. Phys. B: At. Mol. Opt. Phys. **43** 065505 (2010); **43** 215501 (2010).
 - [10] Y. C. Liu, Y. F. Xiao, B. B. Li, X. F. Jiang, Y. Li, and Q. Gong, Phys. Rev. A **84**, 011805(R) (2011).
 - [11] Y. Shen and J. T. Shen, Phys. Rev. A **85**, 013801 (2012).
 - [12] H. J. Carmichael, *Statistical Methods in Quantum Optics I: Master Equations and Fokker-Planck Equations* (Springer-Verlag, Berlin, 2003).
 - [13] J. T. Shen and S. Fan, Phys. Rev. Lett. **95**, 213001 (2005).

- (2005).
- [14] L. Zhou, J. Lu, and C. P. Sun, *Phys. Rev. A* **76**, 012313 (2007).
 - [15] L. Zhou, Z. R. Gong, Y. X. Liu, C. P. Sun, and F. Nori, *Phys. Rev. Lett.* **101**, 100501 (2008).
 - [16] H. Dong, Z. R. Gong, H. Ian, Lan Zhou, and C. P. Sun, *Phys. Rev. A* **79**, 063847 (2009).
 - [17] Y. Chang, Z. R. Gong, and C. P. Sun, *Phys. Rev. A* **83**, 013825 (2011).
 - [18] L. Zhou, Y. Chang, H. Dong, L. M. Kuang, and C. P. Sun, *Phys. Rev. A* **85**, 013806 (2012).
 - [19] J. T. Shen and S. Fan, *Phys. Rev. Lett.* **98**, 153003 (2007); *Phys. Rev. A* **76**, 062709 (2007).
 - [20] D. Roy, *Phys. Rev. A* **83**, 043823 (2011).
 - [21] J. Q. Liao and C. K. Law, *Phys. Rev. A* **82**, 053836 (2010).
 - [22] P. Longo, P. Schmitteckert, and K. Busch, *Phys. Rev. A* **83**, 063828 (2011); *Phys. Rev. Lett.* **104**, 023602 (2010).
 - [23] T. Shi and C. P. Sun, *Phys. Rev. B* **79**, 205111 (2009); arXiv:0907.2776.
 - [24] T. Shi, S. Fan, and C. P. Sun, *Phys. Rev. A* **84**, 063803 (2011).
 - [25] E. Rephaeli and S. Fan, *Phys. Rev. Lett.* **108**, 143602 (2012).
 - [26] E. Rephaeli, Ş. E. Kocabaş, and S. Fan, *Phys. Rev. A* **84**, 063832 (2011).
 - [27] T. Aoki, B. Dayan, E. Wilcut, W. P. Bowen, A. S. Parkins, T. J. Kippenberg, K. J. Vahala, and H. J. Kimble, *Nature* **443**, 671 (2006).
 - [28] T. Yoshie, A. Scherer, J. Hendrickson, G. Khitrova, H. M. Gibbs, G. Rupper, C. Ell, O. B. Shchekin, and D. G. Deppe, *Nature* **432**, 200 (2004).
 - [29] A. Badolato, K. Hennessy, Mete Atatüre, J. Dreiser, E. Hu, P. M. Petroff, and A. Imamoglu, *Science* **308**, 1158 (2005).
 - [30] D. Englund, A. Faraon, I. Fushman, N. Stoltz, P. Petroff, J. Vučković, *Nature* **450**, 857 (2007).
 - [31] K. Hennessy, A. Badolato, M. Winger, D. Gerace, M. Atatüre, S. Gulde, S. Fält, E. L. Hu, and A. Imamoglu, *Nature* **445**, 896 (2007).
 - [32] I. Fushman, D. Englund, A. Faraon, N. Stoltz, P. Petroff, and J. Vučković, *Science* **320**, 769 (2008).
 - [33] P. Michler, A. Kiraz, C. Becher, W. V. Schoenfeld, P. M. Petroff, Lidong Zhang, E. Hu, and A. Imamoglu, *Science* **290**, 2282 (2000).
 - [34] K. M. Birnbaum, A. Boca, R. Miller, A. D. Boozer, T. E. Northup, and H. J. Kimble, *Nature (London)* **436**, 87 (2005).
 - [35] A. Kubanek, A. Ourjoumtsev, I. Schuster, M. Koch, P. W. H. Pinkse, K. Murr, and G. Rempe, *Phys. Rev. Lett.* **101**, 203602 (2008).
 - [36] A. Badolato, M. Winger, K. J. Hennessy, E. L. Hu, A. Imamoglu, C. R. Physique **9**, 850 (2008).
 - [37] J. P. Reithmaier, G. Sek, A. Löffler, C. Hofmann, S. Kuhn, S. Reitzenstein, L. V. Keldysh, V. D. Kulakovskii, T. L. Reinecke, and A. Forchel, *Nature* **432**, 197 (2004).
 - [38] T. Yoshie, A. Scherer, J. Hendrickson, G. Khitrova, H. M. Gibbs, G. Rupper, C. Ell, O. B. Shchekin, and D. G. Deppe, *Nature* **432**, 200 (2004).
 - [39] E. Ginossar, L. S. Bishop, D. I. Schuster, and S. M. Girvin, *Phys. Rev. A* **82**, 022335 (2010).
 - [40] A. Blais, R. S. Huang, A. Wallraff, S. M. Girvin, and R. J. Schoelkopf, *Phys. Rev. A* **69**, 062320 (2004).
 - [41] H. Lehmann, K. Symanzik, and W. Zimmermann, *Nuovo Cimento* **1**, 1425 (1955).
 - [42] F. Marquardt and S. M. Girvin, *Physics* **2**, 40 (2009).
 - [43] P. Zhang, Y. D. Wang, and C. P. Sun, *Phys. Rev. Lett.* **95**, 097204 (2005).
 - [44] F. Xue, L. Zhong, Y. Li, and C. P. Sun, *Phys. Rev. B* **75**, 033407 (2007).
 - [45] P. Rabl, *Phys. Rev. Lett.* **107**, 063601 (2011).